



Missouri University of Science and Technology
Scholars' Mine

International Specialty Conference on Cold-Formed Steel Structures

(1973) - 2nd International Specialty Conference on Cold-Formed Steel Structures

Oct 22nd, 12:00 AM

Bending Strength of Deep Corrugated Steel Panels

James L. Jorgenson

Chingminn Chern

Follow this and additional works at: <https://scholarsmine.mst.edu/isccss>

 Part of the [Structural Engineering Commons](#)

Recommended Citation

Jorgenson, James L. and Chern, Chingminn, "Bending Strength of Deep Corrugated Steel Panels" (1973). *International Specialty Conference on Cold-Formed Steel Structures*. 1. <https://scholarsmine.mst.edu/isccss/2iccfss/2iccfss-session4/1>

This Article - Conference proceedings is brought to you for free and open access by Scholars' Mine. It has been accepted for inclusion in International Specialty Conference on Cold-Formed Steel Structures by an authorized administrator of Scholars' Mine. This work is protected by U. S. Copyright Law. Unauthorized use including reproduction for redistribution requires the permission of the copyright holder. For more information, please contact scholarsmine@mst.edu.

by

James L. Jorgenson¹ and Chingmiin Chern²

1. INTRODUCTION

The corrugated metal panels under study are fabricated from rolled sheet galvanized steel. The fabrication process consists of: unrolling, cutting, punching, and then going through a rollformer which permits the panels to take on the corrugated shape. If curved panels are desired a final operation, stretch forming, is used. This consists of placing the panel in tension and then stretching it around a mold with the desired radius.

These panels are used in the construction of metal buildings. The buildings are either of an arch shape incorporating the curved panels or are planer walls and roof incorporating the straight panels. The metal panels serve as both a covering of the building and as a structural frame.

1.1 Material

The material used for testing was supplied in accordance with ASTM A525 "zinc-coated steel sheets of commercial quality." It is deficient in that the material does not

-
1. Chairman and Professor of Civil Engineering, North Dakota State University, Fargo, North Dakota 58102
 2. Assistant Professor of Civil Engineering, North Dakota State University, Fargo, North Dakota 58102

meet a minimum strength requirement. Future steel should be purchased in accordance with ASTM A 446 which is similar to A 525 only it does satisfy minimum strength requirements.

1.2 Code Evaluation

The usual method of strength evaluation for these panel sections is to apply the criteria of the appropriate building code. The code used here was the "Specification for the Design of Cold-Formed Steel Structural Members", 1968 Edition, by the American Iron and Steel Institute. This section comments on the problems in directly applying the code and suggests that a laboratory testing program is necessary to determine the true strength of the panels.

The allowable bending moment on the panel is dependent on the shape of the panel and the yield strength of the steel. The shape of the panel is shown in Fig. 2. It is proportioned such that each flange permits full effective design width for the compression elements. Using 33 ksi yield steel this will permit a flexural stress of 20 ksi. However, when consideration is given to the deep thin web the allowable flexural stress is significantly reduced. The Code limit for h/t is 200, however, the panel under study has values of 175, 232, 280, and 350 for the 18, 20, 22 and 24 gage panels. When these web thickness ratios are used to determine the allowable bending stress, the values are 16.4, 9.3, 6.4, and 4.1

ksi for the 18, 20, 22, and 24 gage panels. Since these h/t values are outside the range of the code it is doubtful that the resulting code allowable stresses are applicable. Hence, only through a laboratory test can the panel bending strength be evaluated.

Another factor which necessitates testing is the evaluation of the curvature effect on the strength of the panel. The code does not have bending strength criteria for curved panels.

2. TESTING PROGRAM

2.1 Introduction

The testing program consisted of determining the static ultimate strength of the corrugated panels subjected to transverse bending. The thickness of the specimens in four different gages (Gage Nos. 18,20,22, and 24) were used in the testing. A typical specimen diaphragm consisted of three corrugated panels in straight or curved form. The radius of curvature of the curved panels is 30 feet and 6 inches. The dimensions of a typical specimen diaphragm in their horizontal projections are shown in Fig. 1.

A cross-section of the shape of the corrugated panel and its dimensions are shown in Fig. 2. The centroid of the panel section is located at 4.18 inches from the bottom flanges, as shown in the figure. The section is symmetrical with respect to its vertical axis.

The dimensions and gage number of all curved and straight panels with the designation of each test and the corresponding test set-up are provided in Table 1.

2.2 Mechanical Properties of Steel

The steel properties of importance to this investigation are the yield strength, tensile strength and the

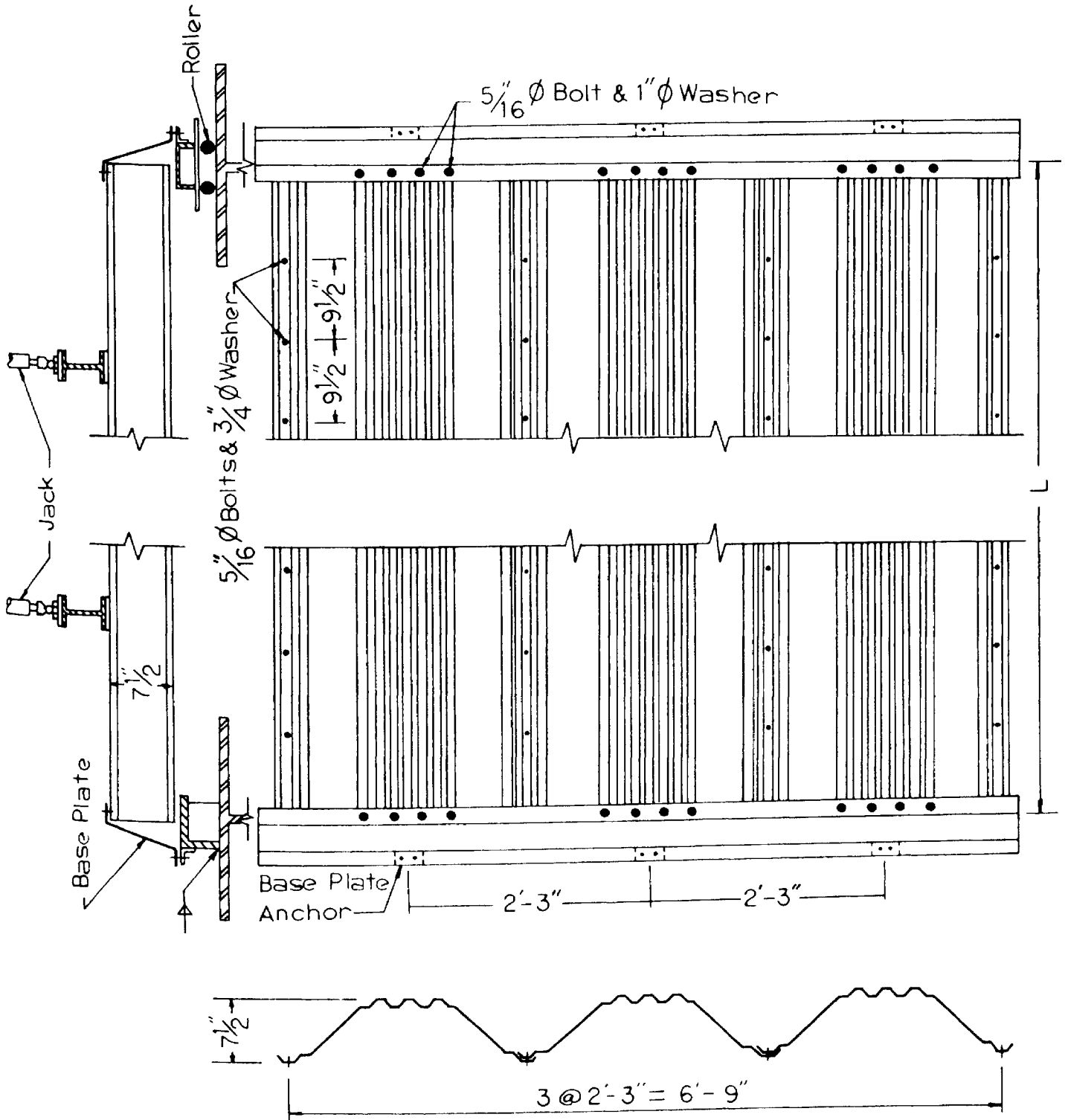
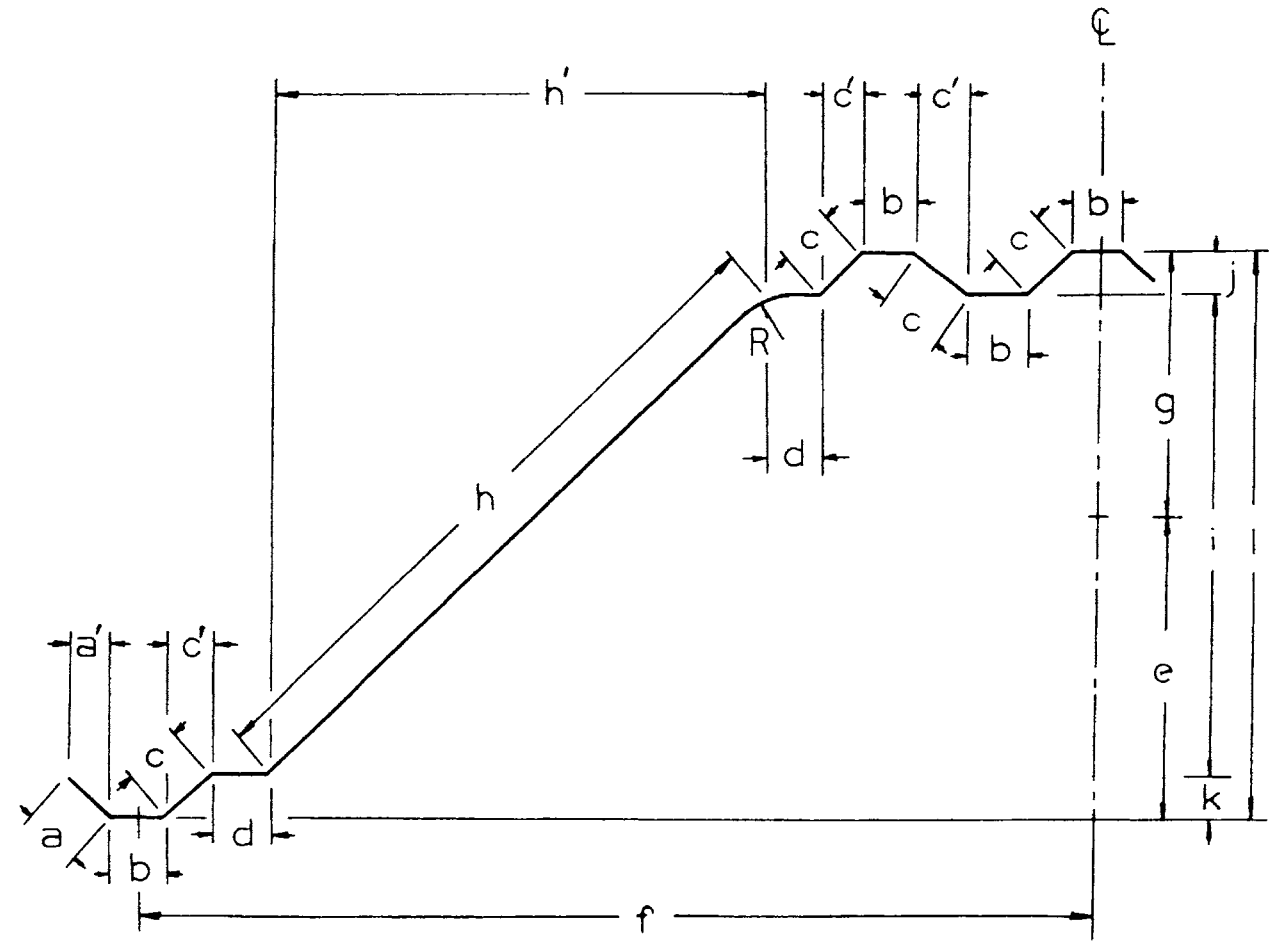


FIG. 1 TYPICAL PANEL TEST SPECIMEN



Unit: Inches

a	a'	b	c	c'	d	e	f	g	h	h'	i	j	k	l	R
.875	.703	.937	.875	.703	.937	4.18	13.50	3.32	8.50	6.00	6.09	.703	.703	7.50	.187

FIG. 2 DIMENSIONS OF CORRUGATED SHAPE

Designation	Gage No.	Length (ft)		Transverse Cross-Section	Test Set-up
		A	L		
BF 1-1	20	4.00	12.33		
BF 2-1	24	4.42	13.26		
BF 3-1	18	3.90	11.70		
BF 4-1	22	4.42	13.26		
BF 1-2	20	4.00	12.33		
BF 2-2	24	4.42	13.26		
BF 3-2	18	3.90	11.70		
BC 1-1	20	4.42	13.26		
BC 2-1	24	4.42	13.16		
BC 3-1	22	4.42	13.26		
BC 1-2	20	4.42	13.26		
BC 2-2	24	3.23	13.26		
BC 3-2	22	5.23	13.26		

TABLE 1 TEST SET UP

percentage elongation at rupture of the steel. This section is devoted to the evaluation of those properties.

Three groups of tensile coupons were cut from each gage of corrugated panels. Each group consisted of at least three coupons. All coupons were cut parallel to the longitudinal direction of the panels. The relative location of the coupons in their respective panels is illustrated in Fig. 3. The dimensions of the tensile coupons, which are provided in Reference 3*, are also shown in the figure. Figure 4 demonstrates a typical stress-strain curve obtained from the tensile coupon tests.

Listed in Table 2 are the test results on each coupon. Columns 2,3 and 4 of the table describe the locations on the corrugated panels from which the corresponding coupons were cut. Further listed from these columns are the static yield point, ultimate tensile strength and the percentage elongation at rupture.

2.3 Loading System

The loading system used in this testing program consisted of a set of four Enerpac hydraulic jacks (Model No. 22-092), connecting to a Riehle pumping and indicating unit (Model M-type Pumping Unit). The hydraulic jack has

*References are listed on page 256.

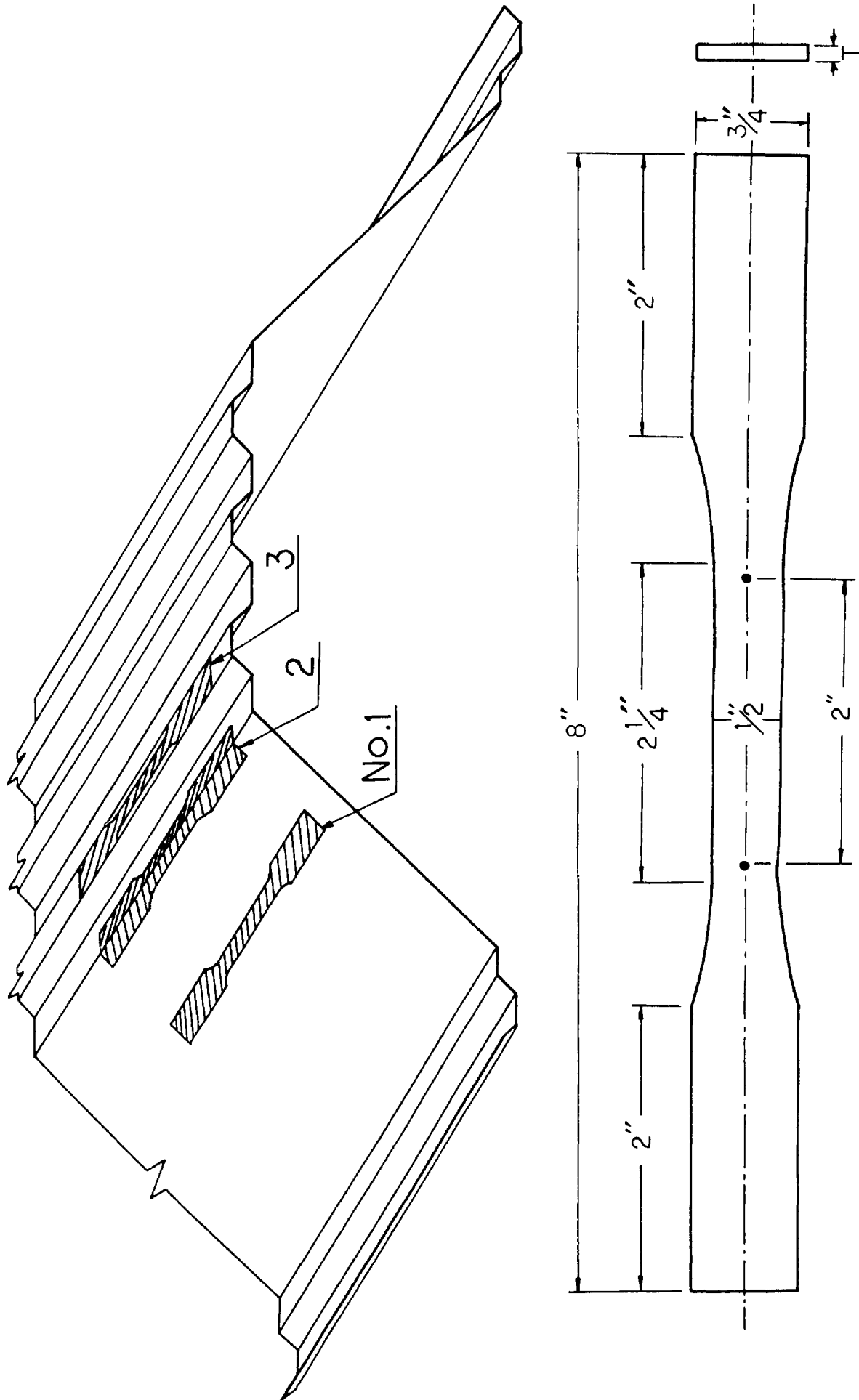


FIG. 3 DIMENSIONS & LOCATION OF COUPONS

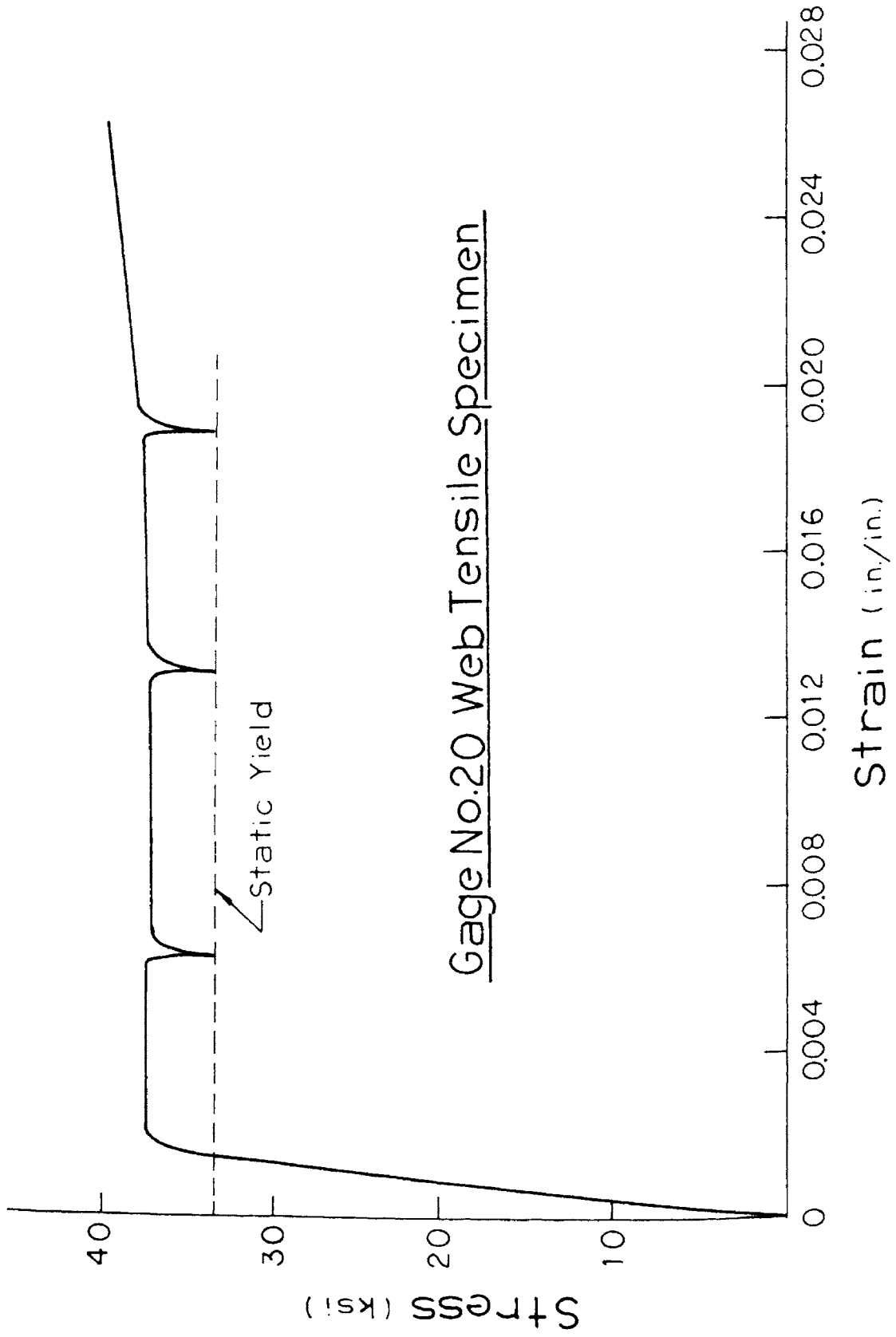


FIG. 4 TYPICAL STRESS-STRAIN DIAGRAM OF COUPONS

Gage No.	1 Web			2 Corner			3 Flange		
	Static Yield (ksi)	Tensile Strength (ksi)	% Elongation	Static Yield (ksi)	Tensile Strength (ksi)	% Elongation	Static Yield (ksi)	Tensile Strength (ksi)	% Elongation
18	35.1	47.6	27.5	38.4	48.0	15.6	34.8	47.7	26.2
	34.3	46.9	27.5	41.5	48.8	17.2	34.0	48.6	24.7
	35.1	46.7	27.5	40.5	49.0	18.4	30.5	47.7	24.7
	ave.	34.8	47.1	27.5	40.1	48.6	17.1	33.1	48.0
20	33.5	48.7	25.2	39.0	50.5	18.7	40.0	51.7	26.7
	34.0	48.7	28.4	39.2	50.5	15.6	37.7	51.5	26.7
	31.6	47.5	25.2	39.0	50.4	15.6	37.7	51.2	25.1
	ave.	33.0	48.3	26.3	39.1	50.5	16.6	38.5	51.5
22	33.0	49.3	26.2	42.0	56.0	15.6	35.9	50.5	23.2
	34.8	50.2	26.2	43.4	55.2	15.6	33.5	49.5	26.4
	34.1	48.8	24.7	42.5	56.5	15.6	35.3	49.5	26.4
	ave.	34.0	49.4	25.7	42.6	55.9	15.6	34.9	49.8
24	38.5	53.6	26.2	40.5	56.7	18.7	42.2	57.0	26.2
	37.0	53.8	24.7	37.3	53.2	18.7	42.2	58.0	26.2
	38.5	53.4	26.2	45.6	53.0	17.2	40.7	56.5	26.2
	ave.	38.0	53.6	25.7	41.1	54.3	18.2	41.7	57.2

TABLE 2 MECHANICAL PROPERTIES OF STEEL

the effective piston area in advance of 1.77 square inches. The Riehle pumping unit is equipped with two 'M'-type gage indicators. The gage indicator used has a range from 0 to 4,000 psi with the scale of 10 psi per division.

2.4 Instrumentation

Locations of dial gages for the readings of the vertical deflection of the corrugated panels were at the one-third, center and two-third points of the span length. Ames dial gages with graduation of one thousandth of an inch were used. The gages were placed in the same locations for all tests.

One dial gage was also installed at the mid-width of the specimen diaphragm at the roller-supported end. The main purpose of this dial gage was to measure the horizontal displacement of the specimen under transverse bending.

2.5 Test Set-up

The test set-up was such that a simply determinate system would result. Details of a typical specimen diaphragm is shown in Fig. 1. One end of the specimen diaphragm was bolted to a 12 gage base plate* which was in turn bolted to a fixed support. The other end of the

*Base plates were supplied by the WEDG-COR, Inc., Jamestown North Dakota.

specimen diaphragm was also bolted to a piece of 12 gage base plate which then rest on the roller support.

The loads were applied through two pairs of the hydraulic jacks to two W 6x8.5 beams which are located at about one-third points of the span from each end. The purpose of the W 6x8.5 beams was to distribute the concentrated jack loads into two uniform line loads across the specimen diaphragm. General views of the test set-up are given in Figs. 5 and 6. When the side flanges of the two exterior panels of the specimen diaphragm were in tension, as shown in Fig. 5, no reinforcement for the side flanges was necessary since it was in tension, the side flange would not have instability problems. However, the edge reinforcement was provided when the side flanges of the specimen diaphragm were in compression, as shown in Fig. 6. The reinforcement was achieved by using a six inch wide sheet metal, which was cut from the other corrugated panels bolted along the side flanges. By using slotted holes in the metal reinforcement, it provided lateral support without increasing compressive strength of the entire specimen diaphragm.

In reality, the building will have a series of corrugated panels connected together to form the walls or roofs. In such a manner the lateral movement of the panels in the direction of the corrugation will be minimized. In order to simulate the above mentioned situa-



FIG. 5 TYPICAL TEST SET-UP (TYPE 1)

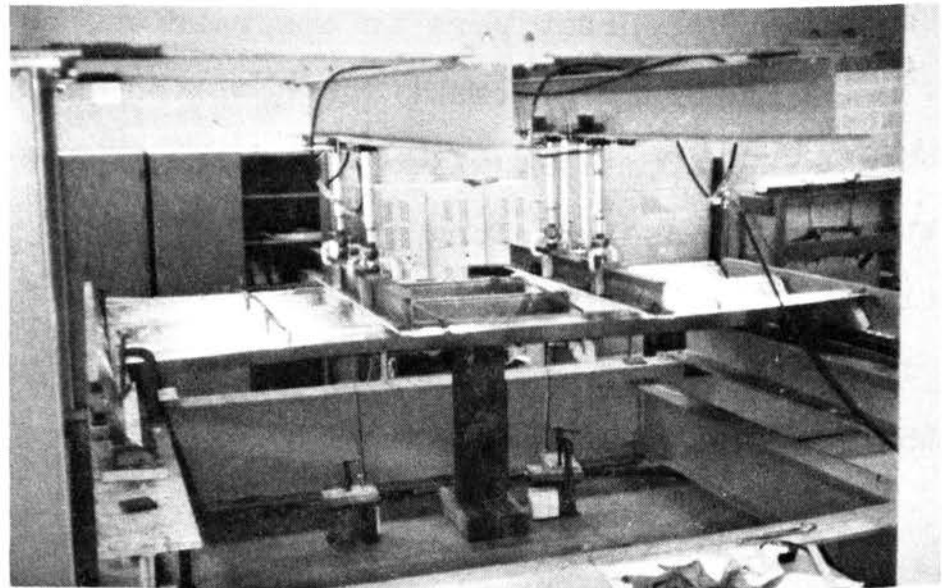


FIG. 6 TYPICAL TEST SET-UP (TYPE 2)

ation in the test specimen, four $3/16$ "x2" mild steel strips were bolted to the exterior side flanges. Figure 6 shows the details of this arrangement.

3. TESTING PROCEDURES AND RESULTS

3.1 Procedures

The first step in the testing procedure was to record all the initial gage deflection readings. Then a certain increment of the load (from 50 to 200 psi) was gradually applied to the specimen diaphragm. The load was held at this value until the readings on the deflection gages were stabilized. The readings on all gages were then recorded. This procedure was repeated for each additional load increment until the deflection was observed increasing without an increase in the applied load. This load was called "the ultimate load".

The results of the tests are expressed in terms of the applied load $2P$ (the loads on a pair of jacks) versus the following parameters: the vertical deflections at the one-third point, mid-span, and two-third point of the span, and the horizontal displacement at the roller-end of the specimen diaphragm.

3.2 General Behavior

The behavior of the corrugated panels subjected to transverse bending followed the same general pattern. The first noticeable distress was the formation of the wrinkle shape on the panel webs. The second was the buckling of

the compression flanges at or near the locations of the applied loads. The amount of buckling increased with loads. The third noticeable behavior was the failure mode which was marked by a significant increase in the vertical deflection and decrease in load-carrying capacity. Failure was generally caused by excessive buckling at the junction of the panel web and compression flange of the specimen diaphragms.

The behavior of each test specimen is demonstrated in the load-deflection diagrams. Typical load-deflection diagrams for the specimen diaphragms consisted of straight corrugated panels, and of curved corrugated panels are illustrated, respectively, in Figs. 7 and 9. As shown in the figures, dial gage Nos. 1 and 3 indicated the vertical deflections at the one-third points of the span. Dial gage No. 2 was for the measurement of the vertical deflection at the mid-span. Gage No. 4 was for the horizontal displacement of the specimen diaphragm.

The loading procedures and the failure modes were in a similar manner for all specimen diaphragms with straight or curved panels. Items of particular interest on those specimens are listed as follows:

BF 1-1 (Gage 20)

The load was gradually increased at 200 psi intervals

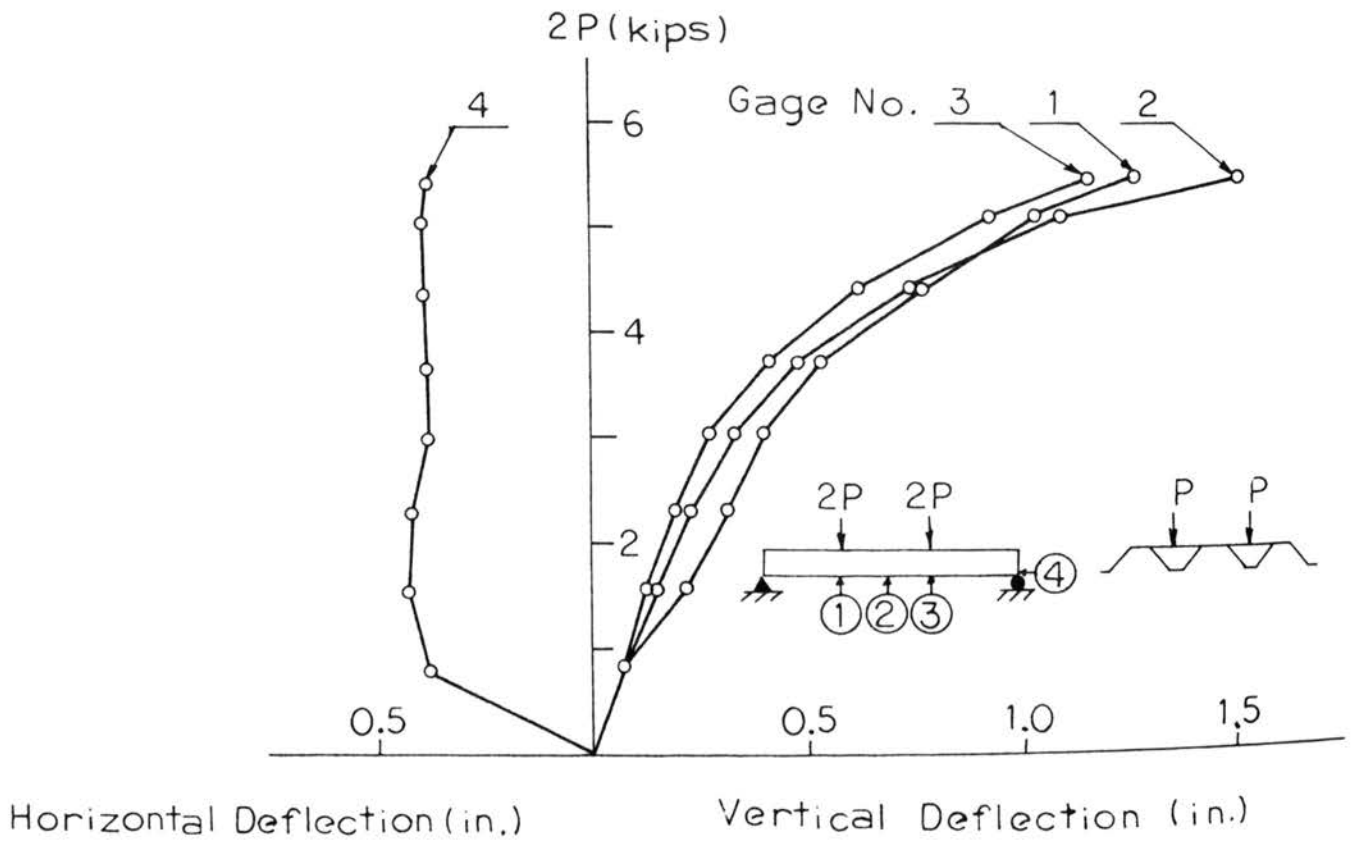


FIG. 7 LOADING DIAGRAM (BF 1-1)

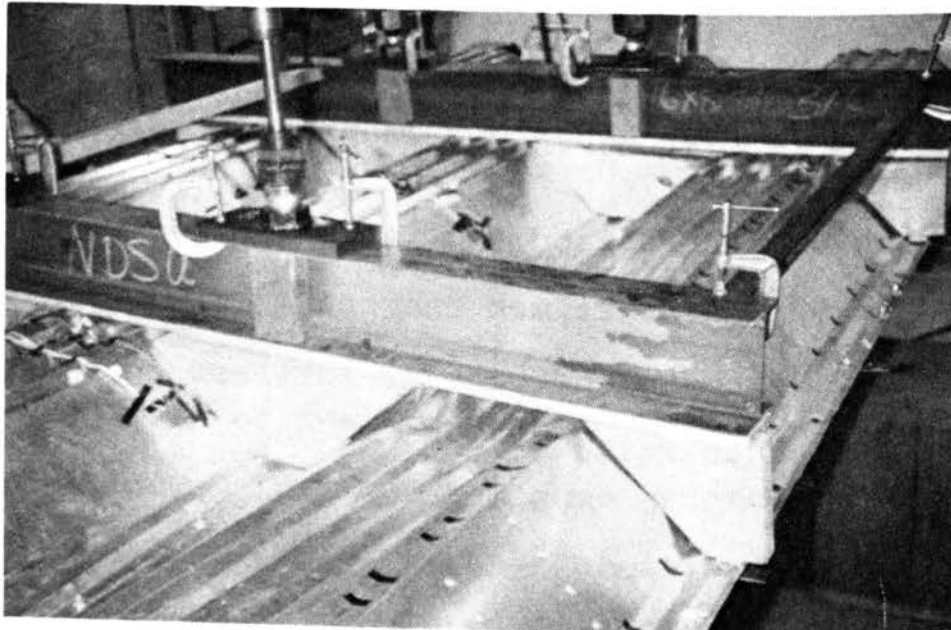


FIG. 8 BF 1-1 AFTER FAILURE

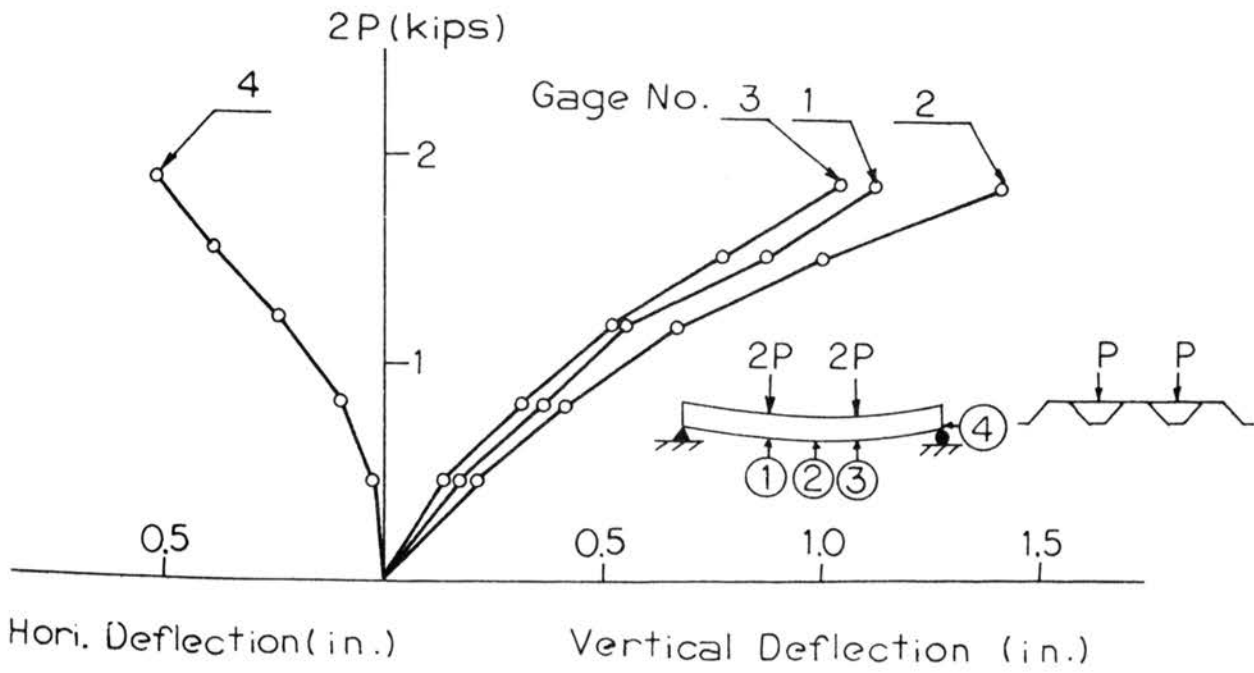


FIG. 9 LOADING DIAGRAM (BC 3-1)

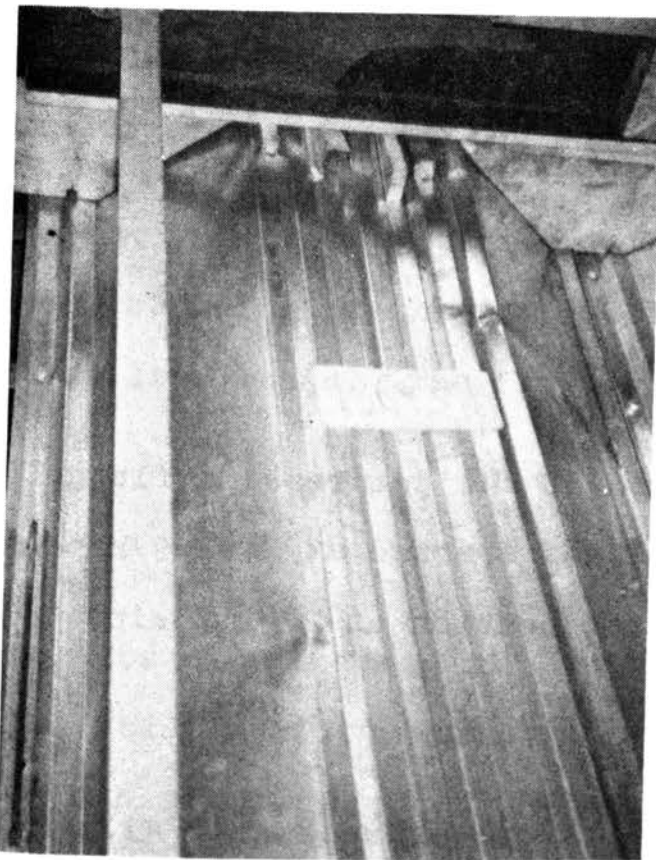


FIG. 10 BC 3-1 AFTER FAILURE

($2P=0.825$ kip per pair of jacks). At $2P=2.26$ kips, the lateral bracing strips ($3/16" \times 2"$) between outside flanges bowed. At $2P=3.60$ kips, the compression flange at the mid-span portion bowed upward. At $2P=5.10$ kips, the compression flanges buckled at the locations of applied loads. With the load held at $2P=5.40$ kips the deflection continued to increase and thus the ultimate bending capacity of the diaphragm was reached. The load-deflection diagram of test BF 1-1 is shown in Fig. 7. The characteristics of the specimen diaphragm after failure is shown in Fig. 8.

BF 1-2 (Gage 20)

Downward bowing of the compression flanges near the loading points was noticed at about $2P=2.90$ kips. At $2P=3.30$ kips, pronounced deformations were observed at the same locations. The diaphragm was unable to carry further applied load.

BF 2-1 (Gage 24)

Downward bowing of the compression flange near the points of applied loads started at $2P=1.9$ kips and failure occurred at the same location at $2P=2.2$ kips.

BF 2-2 (Gage 24)

Wrinkles were noticed on webs at $2P=1.9$ kips. The downward buckling of the compression flanges at the mid-span occurred at $2P=2.5$ kips.

BF 3-1 (Gage 18)

Wrinkles started on webs at $2P=3.3$ kips and failure occurred at $2P=7.0$ kips at the locations of applied loads.

BF 3-2 (Gage 18)

Wrinkles appeared on webs at $2P=3.3$ kips and failure occurred at the mid-span at $2P=4.0$ kips.

BF 4-1 (Gage 22)

Downward bowing of the compression flanges near the location of applied loads started at $2P=2.9$ kips and failure occurred at the mid-span at $2P=3.5$ kips due to upward buckling of the compression flanges.

BC 1-1 (Gage 20)

At $2P=2.0$ kips, wrinkles appeared at the panel webs and failure due to buckling of the compression flanges near one of the applied line loads. The failure load was $2P=2.8$ kips.

BC 1-2 (Gage 20)

Wrinkles on webs were noticed at $2P=2.8$ kips. Pronounced downward buckling of the compression flanges at the mid-span portion was observed at $2P=3.9$ kips.

BC 2-1 (Gage 24)

Wrinkles appeared on webs at $2P=1.2$ kips and then at $2P=1.5$ kips failure occurred near one of the applied line loads due to downward buckling of the compression flanges.

BC 2-2 (Gage 24)

Wrinkles appeared on webs at $2P=1.2$ kips. The diaphragm failed due to downward buckling of the compression flanges near one of the applied loads.

BC 3-1 (Gage 22)

The load-deflection diagram of test BC 3-1 is shown in Fig. 9. It would represent a typical load-deflection behavior of the specimen diaphragms with curved corrugated panels under transverse bending. In this test, the webs started to form some visible wrinkles at $2P=1.2$ kips. The failure load was attained at $2P=2.1$ kips. The mode of failure of specimen BC 3-1 is shown in Fig. 10.

BC 3-2 (Gage 22)

Wrinkles started to appear on webs at the load of $2P=2.2$ kips. The failure load was attained at $2P=3.3$ kips due to downward buckling of the compression flange under one of the applied loads.

The results of the above mentioned bending tests are summarized in Table 3. Columns 1 and 2 of the table

Gage No.	Designation	Failure Values				Test Set-up & Failure Location
		Moment (ft-kip/ft)	Bending Stress (ksi)	Shear (kip/ft)	Shearing Stress (ksi)	
18	BF 3-1	3.72	25.02	0.95	2.64	
18	BF 3-2	3.30	28.54	0.83	2.30	
20	BF 1-1	3.21	29.32	0.80	2.90	
20	BF 1-2	2.94	33.75	0.73	2.70	
20	BC 1-1	1.95	17.81	0.44	1.62	
20	BC 1-2	2.20	25.95	0.51	1.88	
22	BF 4-1	2.22	24.35	0.50	2.21	
22	BC 3-1	1.33	14.59	0.30	1.33	
22	BC 3-2	1.54	21.21	0.30	1.33	
24	BF 2-1	1.27	17.45	0.29	1.59	
24	BF 2-2	1.28	22.00	0.29	1.60	
24	BC 2-1	0.84	11.48	0.19	1.05	
24	BC 2-2	0.89	15.33	0.28	1.52	

TABLE 3 BENDING TEST RESULTS

give the thickness of the specimen diaphragms in terms of gage numbers and their corresponding test designations. Column 3 lists the failure values of each test. These values were calculated using the jack failure load and the statics of the test specimens on the assumption that each of the component panels carried the same amount of loads. A further correction was to base all test results on material with a static yield strength of 33 ksi for the web specimen. The average yield value for each gage as reported in Table 2 was used. The failure bending moments and the corresponding bending stresses were obtained based on the full section modulus of the corrugated panel. The shear loads and shear stresses are also given for the corresponding bending failure loads. The last column of Table 3 shows the shapes of the specimen diaphragms in which they were arranged and the locations of the failure for each test.

4. DISCUSSION OF TEST RESULTS

A discussion of the test results is contained in the following paragraphs in accordance with the respective headings.

4.1 Moment Capacities (Straight versus Curved Panels)

Even though the member cross-section is the same, there is an apparent difference in moment capacities for diaphragms with curved panels and those with straight panels. This is illustrated in Table 4. The moment capacities for those specimens with the wider flanges in compression resulted in an average of about 62% of the failure moment for the diaphragms with straight panels. On the other hand, the curved diaphragms with the narrower flanges in compression, the average failure moment value is about 73% of those with straight panels.

Why do curved panels fail at a lower load than do straight panels? The reason may be drawn from the curvature effect of the stability of a compression member. Examining the web behavior of all tests described in Art. 3.2, General Behavior, it can be found that the panel web under loads will buckle out of its plane and thus lose its load-carrying capacity. This web buckle-out-of-plane behavior results in the so called "stress re-distribution" in thin skin structures and hence the compressive force on


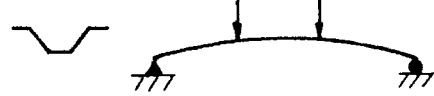

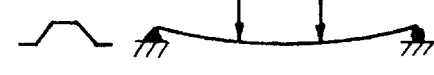
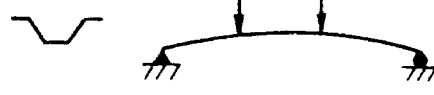
Gage Number	Test Set-up	$\frac{M_f \text{ (Curved Member)}}{M_f \text{ (Straight Member)}}$
20		0.60
20		0.77
22		0.60
24		0.66
24		0.70

TABLE 4 FAILURE MOMENT RATIO (CURVED VS. STRAIGHT MEMBERS)

the entire panel section has to be carried by the compression flange. In other words, the compression flange of the panel will behave like a compression member. It is thus understood that the curvature effect on a compression member will decrease its load-carrying capacity.

4.2 Effect of Panel Thickness on Moment Capacities

The effect of panel thickness on the moment capacities of the specimen diaphragms is illustrated in Fig. 11 where panel thickness is plotted as the abscissa and the failure bending moment as the ordinate. It is seen that the moment capacity of the diaphragms increase as the panel thickness increases. The moment-thickness relationship is seen to be approximately linearly related in these 13 tests. The moment capacity is greater for the thicker panels.

4.3 Effect of Panel Thickness on Bending Stresses

If the failure moment values are divided by the corresponding section modulus of the full panel section, Fig. 11 can then be converted into Fig. 12. The ordinate in the figure is the failure bending stresses of the compression flange which is in accordance with the failure moment values shown in Fig. 11. As shown in Fig. 12, in the 20 to 24 gage range, the failure bending stress increases linearly with panel thickness.

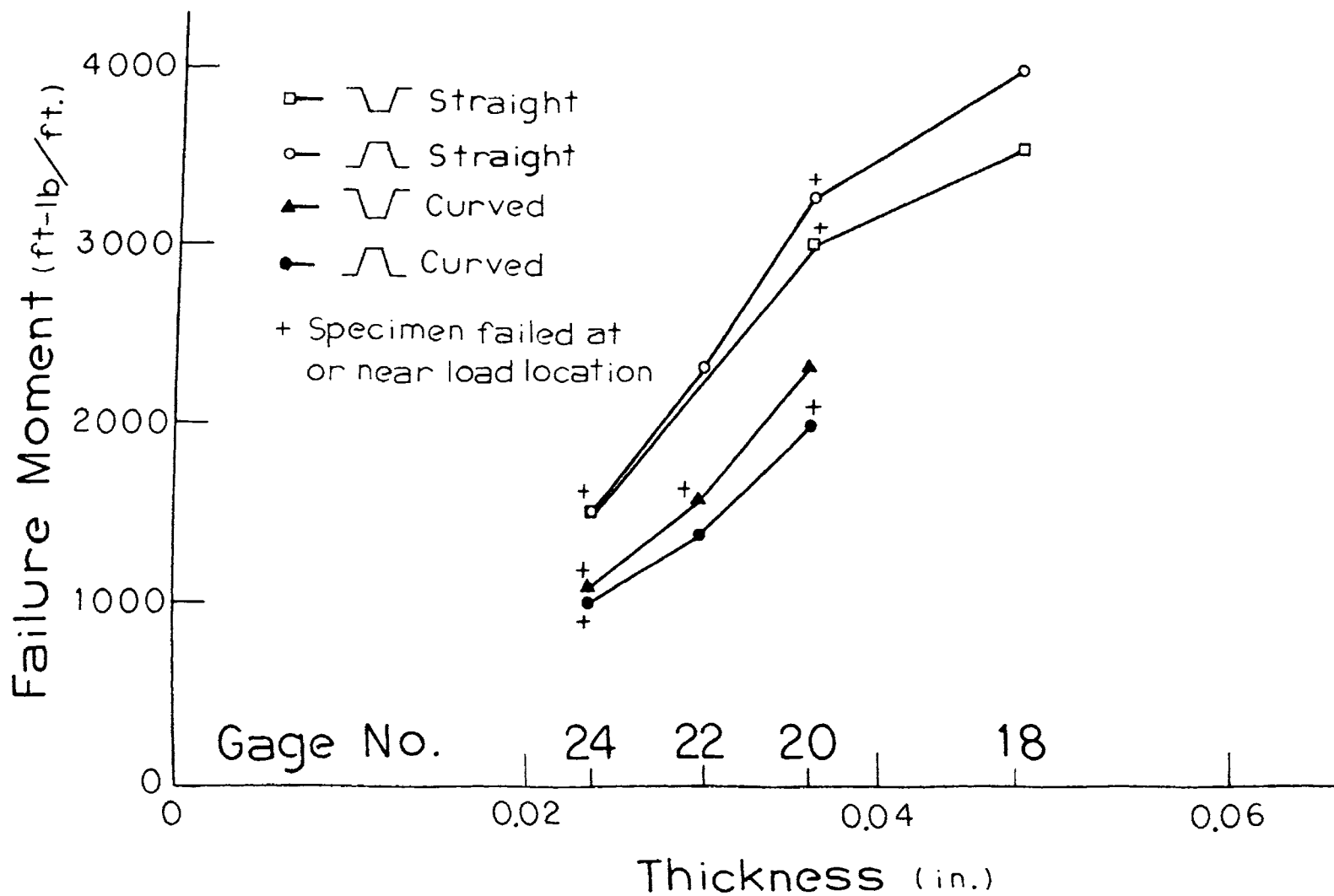


FIG. 11 PANEL THICKNESS VERSUS FAILURE MOMENT

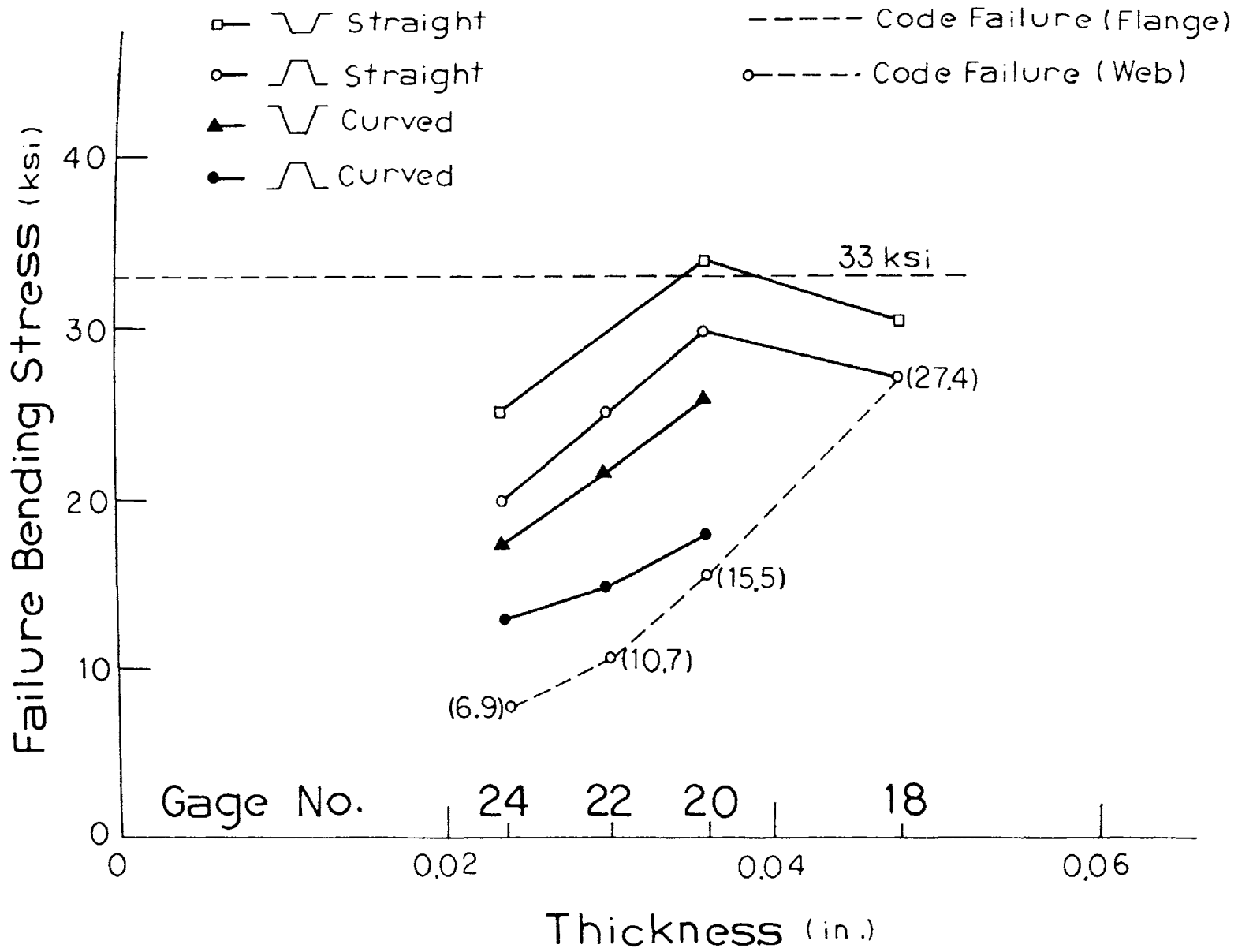


FIG. 12 PANEL THICKNESS VERSUS FAILURE BENDING STRESS

Figure 12 can also be used to compare the actual failure bending stress with that predicted by the code. The 33 ksi line is 1.67 times the allowable bending stress, 20 ksi, based solely on the flange properties. The values in parenthesis are 1.67 times the allowable bending stress in the web as noted in section 1.2 of this report. The comparison suggests that in all but one case the flange criteria is slightly too high, however, except possibly for the curved panels, the web criteria is exceptionally low.

4.4 Effect of Line Loading

As noted in Chapter 2, the panels were loaded with a line load. In practice, a more common loading would be for the load to be uniformly or linearly distributed over the entire surface of the panel. Has the presence of the more concentrated line loads caused premature failure of the diaphragms? If all panels had failed at the location of the concentrated loads, the answer would be yes. Table 3 indicates the location of failure. In only half the tests did failure occur near the line load. When these specimens that did fail near the load locations are noted on Fig. 11, it can be observed that these points are not significantly above or below the fairly straight lines generated by the other points. It is concluded that the presence of the line loads did not significantly reduce the failure bending stress for the members.

5. CONCLUSIONS

The purpose of this research was to determine experimentally the behavior of light gage cold-formed steel panels subjected to transverse bending. The conclusions drawn from this investigation may be summarized as follows:

1. Failure of the specimen diaphragms in transverse bending was initiated by local buckling at the junctions of the compression flange and adjacent webs.
2. The code criteria for allowable bending stress in the web is extremely conservative when applied for h/t values above the 200 limit.
3. The curved panel specimens failed at between 60% and 77% of the moment values for the identical straight panel specimens.
4. Higher failure moment values were observed when the wider flange was in compression (as compared to those with the narrower flanges in compression) for specimens with straight panels but were less for those with curved panels.
5. The moment capacity increases almost linearly with increase in panel thickness.

REFERENCES

1. American Institute of Steel Construction
SPECIFICATION FOR DESIGN, FABRICATION, AND ERECTION
OF STRUCTURAL STEEL FOR BUILDING, AISC, New York,
1971
2. American Iron and Steel Institute
SPECIFICATION FOR THE DESIGN OF COLD-FORMED STEEL
STRUCTURAL MEMBERS, 1968 Edition, AISI, New York
1970
3. American Society for Testing and Materials
ANNUAL BOOK OF ASTM STANDARDS, Part 3, ASTM, 1970
4. Sukhatunga, P.
STRENGTH OF LIGHT GAGE COLD-FORMED STEEL PANELS, M.S.
Paper, Department of Civil Engineering, North Dakota
State University, August 1972
5. Winter, G.
COMMENTARY ON THE 1968 EDITION OF THE SPECIFICATION
FOR THE DESIGN OF COLD-FORMED STEEL STRUCTURAL MEMBERS,
AISI, New York, 1970

ACKNOWLEDGMENTS

This research work was sponsored by a metal building firm, WEDG-COR, INC. of Jamestown, North Dakota. Most of the laboratory work was performed by a former Graduate Assistant in Civil Engineering, Pramote Sukhatunga.

SUMMARY

Experiments on full size specimens were conducted to investigate the bending strength of light gage cold formed steel panels. Local buckling at the compression flange and web junction initiated the bending failure. The code criteria for allowable bending stress in the web is extremely conservative when applied to web-depth to thickness ratios above the 200 limit.